Cell, Vol. 93, 189–201, April 17, 1998, Copyright ©1998 by Cell Press

Fulminant Jejuno-Ileitis following Ablation of Enteric Glia in Adult Transgenic Mice

Toby G. Bush,[1,2,7] Tor C. Savidge,[1,3]
Tom C. Freeman,[4] Hilary J. Cox,[1]
Elizabeth A. Campbell,[4] Lennart Mucke,[5]
Martin H. Johnson,[2] and Michael V. Sofroniew[1,2,6]
[1]Medical Research Council Cambridge Centre
for Brain Repair
Forvie Site, Robinson Way
Cambridge CB2 2PY
[2]Department of Anatomy
University of Cambridge
Downing Street
Cambridge CB2 3DY
[3]Institute of Child Health
University of Birmingham
Birmingham, BI6 8ET
[4]Sanger Centre
Wellcome Trust Genome Campus
Hinxton CB10, 1SA
United Kingdom
[5]Gladstone Molecular Neurobiology Program
and Department of Neurology
University of California
San Francisco, California 94141-9100

Summary

To investigate the roles of astroglial cells, we targeted their ablation genetically. Transgenic mice were generated expressing herpes simplex virus thymidine kinase from the mouse glial fibrillary acidic protein (GFAP) promoter. In adult transgenic mice, 2 weeks of subcutaneous treatment with the antiviral agent ganciclovir preferentially ablated transgene-expressing, GFAP-positive glia from the jejunum and ileum, causing a fulminating and fatal jejuno-ileitis. This pathology was independent of bacterial overgrowth and was characterized by increased myeloperoxidase activity, moderate degeneration of myenteric neurons, and intraluminal hemorrhage. These findings demonstrate that enteric glia play an essential role in maintaining the integrity of the bowel and suggest that their loss or dysfunction may contribute to the cellular mechanisms of inflammatory bowel disease.

Introduction

Astroglia are among the most numerous cells in all neural systems. Many aspects of their functions are not well understood. To investigate the roles of astrocytes and related astroglia in the central (CNS) and peripheral nervous systems, we targeted their cell death genetically using the promoter of glial fibrillary acidic protein (GFAP), an intermediate filament protein (Eddleston and Mucke, 1993). Mouse *Gfap* promoter sequences have been identified, which target reporter gene expression specifically to astroglia, and have been used to express heterologous genes in transgenic mice (Toggas et al., 1994; Johnson et al., 1995). To achieve cellular ablation, we used the thymidine kinase gene of the herpes simplex virus (HSV-*Tk*). Proliferating cells that express transgene-derived HSV-TK metabolize the antiviral agent ganciclovir (GCV) to toxic nucleotide analogs, which disturb nucleic acid synthesis and induce cell death (Frank et al., 1984; Borrelli et al., 1989; Heyman et al., 1989). Thus, cell ablation can be regulated in a regionally and temporally specific manner by where and when GCV is administered.

We report here that in transgenic mice expressing HSV-TK from the mouse *Gfap* promoter, the pattern and regulation of transgene-derived HSV-TK expression is similar to that of endogenous GFAP, and that transgenic astrocytes are vulnerable to GCV in vitro and after CNS injury in vivo. During initial in vivo studies, we found that subcutaneous (s.c.) GCV delivery to uninjured adult transgenic mice was invariably fatal within 19 days in the absence of CNS pathology. We examined vital peripheral organs for expression of transgene-derived HSV-TK and for pathological changes. RT-PCR screening of transgenic mice revealed expression of *Gfap* and HSV-*Tk* in gut, heart, lung, liver, kidney, adrenal, and spleen. Histopathological examination of these organs in transgenic animals receiving GCV revealed major changes only in the gastrointestinal (GI) tract, which showed severe inflammation and necrosis of the jejunum and ileum. Our investigations show that this pathology is related to the ablation of GFAP-expressing enteric glia.

Results

Generation of HSV-TK Expressing Transgenic Mice

Progeny resulting from the pronuclear injection of a *Gfap*-HSV-*Tk* fusion gene construct were screened for successful integration of the transgene (Figures 1A and 1B). Transgenic lines were established from three founder mice. Of these, line 7.1 showed the highest expression of HSV-TK protein in the brain. Densitometry of Southern blots estimated the number of copies of transgene incorporated into the genome of transgenic progeny of line 7.1 to be over 50. Males of line 7.1 were infertile in agreement with previous reports of male sterility in transgenic mice expressing HSV-TK from other promoters (Al-Shawi et al., 1988). All experimental animals were generated by mating heterozygous females of line 7.1 with wild-type males, followed by genotyping by Southern blot and immunohistochemical demonstration of HSV-TK expression. Thus, transgenic and nontransgenic control animals had similar genetic backgrounds.

Production of HSV-TK protein by transgenic mice was demonstrated by Western blot of whole brain extracts (Figure 1C) and immunohistochemistry. HSV-TK was present only in cells with the appearance of astrocytes (Figures 1D and 1E). In double-labeling studies, HSV-TK was always colocalized with GFAP in uninjured mice

[6]To whom correspondence should be addressed.
[7]Present address: Babraham Institute, Babraham, CB2 4AT, United Kingdom.

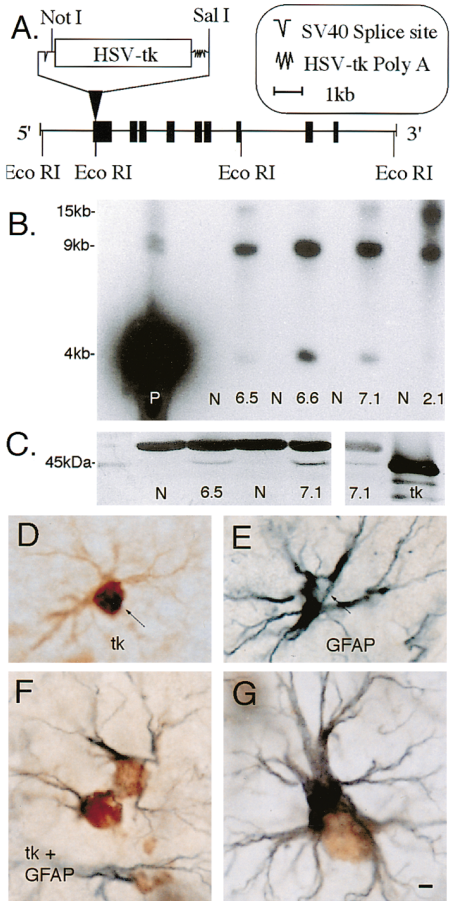

Figure 1. In Vivo Expression of the *Gfap*-HSV-*Tk* Transgene

(A) Fusion gene construct of HSV-*Tk* inserted into exon 1 of the mouse *Gfap* gene.

(B) Southern blot of EcoRI-digested genomic DNA from founder mice (numbers) and nontransgenic littermates (N) hybridized with an HSV-*Tk* probe. P, control plasmid.

(C) Western blot of whole brain extracts from transgenic and nontransgenic (N) progeny of founder lines 6.5 and 7.1. HSV-TK-purified protein (TK) migrates at 45 kDa, with two minor bands 42–44 kDa. A large nonspecific band was present in all brain extracts at 48 kDa.

(D–G) Immunohistochemistry of hippocampal astrocytes in transgenic mice, untreated (D–F), or after stab injury (G). Scale bar = 3 μm. (D) Brown single-color staining of HSV-TK heavily labels soma and nucleus (arrow). (E) Blue single-color staining of GFAP labels fibrous processes while soma and nucleus are unstained (arrow). (F and G) Two-color staining of HSV-TK (brown) and GFAP (blue) shows that brown-stained cell bodies and blue-stained processes belong to the same cells.

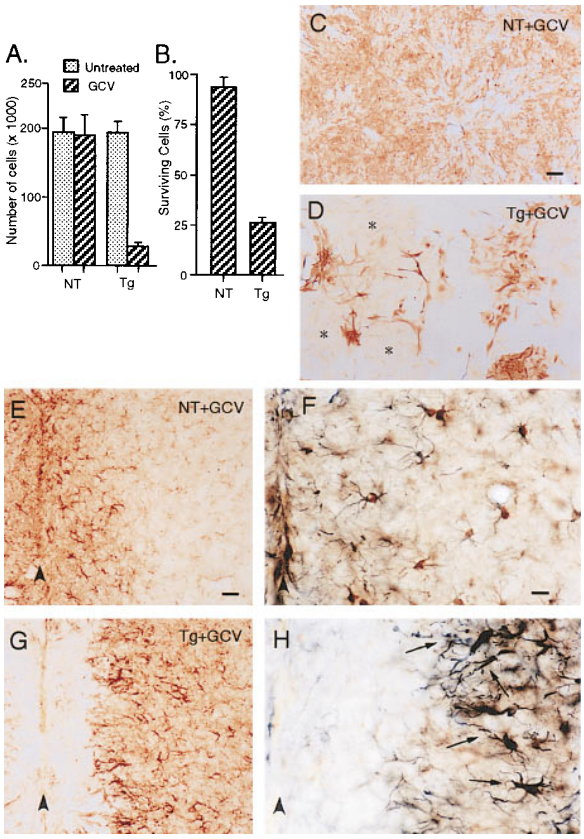

Figure 2. Vulnerability of Transgenic Astrocytes to GCV in Vitro and after Injury In Vivo

(A and B) Cell numbers (MTT assay) in primary astrocyte cultures. (A) Typical experiment. GCV (2 μM, 7 days) significantly ($p < 0.001$) reduced cell number in sister culture wells ($n = 3$) from a transgenic mouse (Tg) but not its nontransgenic (NT) littermate. (B) Cumulative results from 12 transgenic and 12 nontransgenic culture experiments as in (A). GCV significantly reduced the mean number of cells from transgenic, but not nontransgenic, mice by 75% (ANOVA, $p < 0.001$).

(C and D) Immunohistochemistry of GFAP in GCV-treated primary astrocyte cultures. Scale bar = 100 μm. (C) Nontransgenic. Most but not all cells are GFAP-positive. GCV had no effect on cell number or appearance. (D) Transgenic littermate to (C) showing severe loss of GFAP-positive cells and relative increase in GFAP-negative cells (asterisk).

(E–H). Immunohistochemistry of GFAP (brown) alone (E and G) or double-staining for GFAP (blue) plus HSV-TK (brown) (F and H) in the forebrain of GCV-treated mice 14 days after stab injury (arrowheads). Scale bar for (E) and (G) = 35 μm; for (F) = 12 μm. (E and F) Nontransgenic. GCV had no effect on astrocyte scar formation. (G and H) Transgenic. GCV has depleted astrocytes from the wound margins. Neighboring astrocytes have upregulated GFAP and appear swollen and fragmented (arrows in [H]).

or after stab injury to the forebrain, which increased the number, size, and staining intensity of reactive astrocytes (Figures 1F and 1G). HSV-TK was undetectable in nontransgenic littermates.

GCV Mediated Killing of GFAP-HSV-TK Transgenic Astrocytes In Vitro and after Brain Injury In Vivo

The vulnerability of transgenic astrocytes to GCV was tested in vitro using enriched, subconfluent astrocyte cultures from individual neonatal mice, in which about 80% of cells were GFAP-positive. Exposure to GCV for at least 7 days caused a mean cell loss of 75% in cultures from transgenic mice but not their nontransgenic littermates (Figures 2A and 2B). Immunohistochemistry confirmed the specific loss of GFAP-positive cells and showed a relative increase in GFAP-negative cells in GCV-treated transgenic cultures (Figures 2C and 2D). These findings show that astrocytes from transgenic mice, but not their nontransgenic littermates, were killed by GCV in vitro, and that diffusion of toxic metabolites

of GCV produced by transgenic cells was not lethal to neighboring GFAP-negative cells.

The ability of s.c. GCV to kill astrocytes in vivo was tested after stab injury to the brain, a procedure known to upregulate GFAP expression and cause astrocyte proliferation (Eddleston and Mucke, 1993). Because in vitro experiments indicated that prolonged exposure to GCV was needed to achieve substantial ablation of transgenic astrocytes, GCV was delivered continuously in vivo by s.c. osmotic minipump. The astrocytic reaction and glial scar induced by stab injury to the forebrain were robust in GCV-treated nontransgenic mice or untreated transgenic or nontransgenic mice (n = 3–6 mice per group) (Figures 2E and 2F). In contrast, transgenic mice treated with GCV for 7 or 14 days (n = 6 per group) exhibited markedly fewer GFAP and HSV-TK immunoreactive astrocytes adjacent to the wound (Figures 2G and 2H). The pattern of immunohistochemical staining at 7 and 14 days suggested that the GCV-induced death of astrocytes next to the wound margin triggered an astrocytic reaction in adjacent tissue, where many astrocytes looked fragmented, abnormal, and in an early stage of cell death (Figures 2G and 2H).

Fatality of Chronic s.c. GCV Delivery to Transgenic Mice

When continuous s.c. GCV treatment was attempted for longer times, transgenic mice became ill and died within 19 days. This occurred whether or not they had received a brain injury, and in the absence of weight loss (Figures 3A and 3B). There was no evidence of ptosis, suggesting normal function of the superior cervical ganglion and sympathetic nervous system, a site of GFAP expression in peripheral glial cells. The only external signs of illness were reduced activity and scruffing of the fur. The illness showed a fulminating course that was rapidly fatal. Moribund animals were killed in accordance with animal welfare regulations, and tissue collected for analysis.

Transgenic mice treated with GCV for 7 days and discontinued (n = 6) survived for 35 days after the start of GCV (the longest time monitored) and looked healthy. Transgenic mice treated with GCV for 14 days and discontinued (n = 6) became terminally ill by day 18 after the start of GCV, indicating that the lethal changes induced in these mice became irreversible between days 7 and 14. In contrast, s.c. GCV administered continuously for 28 days (the longest time studied) had no detectable effects on nontransgenic animals (n = 6) (Figures 3A and 3B).

To look for potential causes of death, we examined the CNS in detail, in particular vital centers in the hypothalamus and brainstem. Uninjured transgenic mice that received s.c. GCV for 14–17 days (n = 9) showed little or no increase in GFAP-immunoreactivity and no evidence of astrocyte loss or neuronal damage throughout the CNS, compared with similarly processed control mice (Figures 3C–3J).

In the absence of an obvious cause of death due to CNS dysfunction, we looked for other sites that might account for lethality. RT-PCR screening revealed expression of *Gfap* and HSV-*Tk* in major organs including heart, lung, liver, spleen, adrenal, kidney, and GI tract,

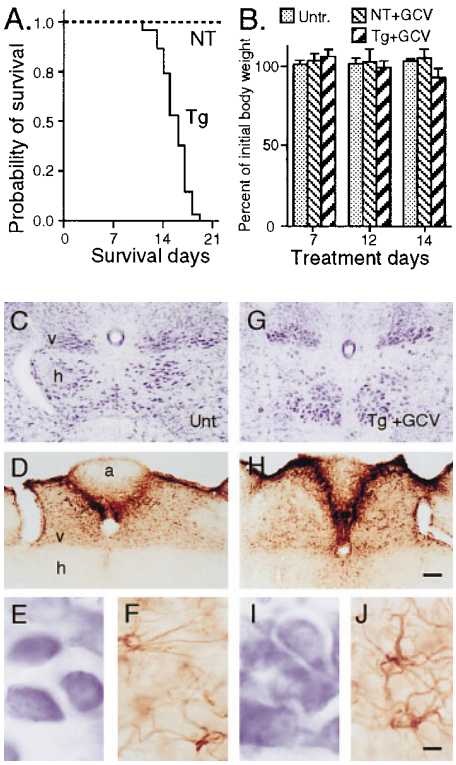

Figure 3. Mortality, Body Weight, and Brain Histology of Transgenic and Nontransgenic Mice Given Continuous s.c. GCV

(A) Probability of survival was not altered by GCV in nontransgenic (NT) mice but fell steeply in transgenic (Tg) mice after 13 days to reach 0 by 19 days.

(B) Fourteen days of GCV caused less than 7% loss of initial body weight in transgenic mice.

(C–J) Cresyl violet staining and immunohistochemistry for GFAP show no difference in the appearance of neurons (C, E, G, and I) and astrocytes (D, F, H, and J) in the medulla of untreated (Unt) nontransgenic (C–F) and moribund GCV-treated transgenic mice (G–J). Scale bar for (C), (D), (G), and (H) = 80 μm; for (E), (F), (I), and (J) = 5 μm.

as well as in neural tissues such as brain and trigeminal ganglion (Figure 4A). No gross or histopathological abnormalities were detected in any major organ in untreated transgenic mice (n = 4 per group) or in nontransgenic mice given GCV for 14 days. Transgenic mice given GCV for 14 days (n = 8) also showed no obvious structural changes to lung, heart, pancreas, kidney, liver, adrenal, spleen, stomach, or colon. However, these mice exhibited pronounced macroscopic changes of the small intestine in all cases (Figures 4C–4H), which correlated with a depletion of *Gfap* and HSV-*Tk* mRNA from the small intestine but not other vital organs (Figures 4A and 4B). The GI tract was therefore studied in greater detail.

Pronounced Inflammation and Necrosis of the Jejunum and Ileum, Severe Blood Loss, and Positive Blood Cultures in GCV-Treated Transgenic Mice

Macroscopic and microscopic examination of the GI tract in untreated transgenic mice (n = 6) or in nontransgenic mice receiving GCV for 11 or 14 days (n =

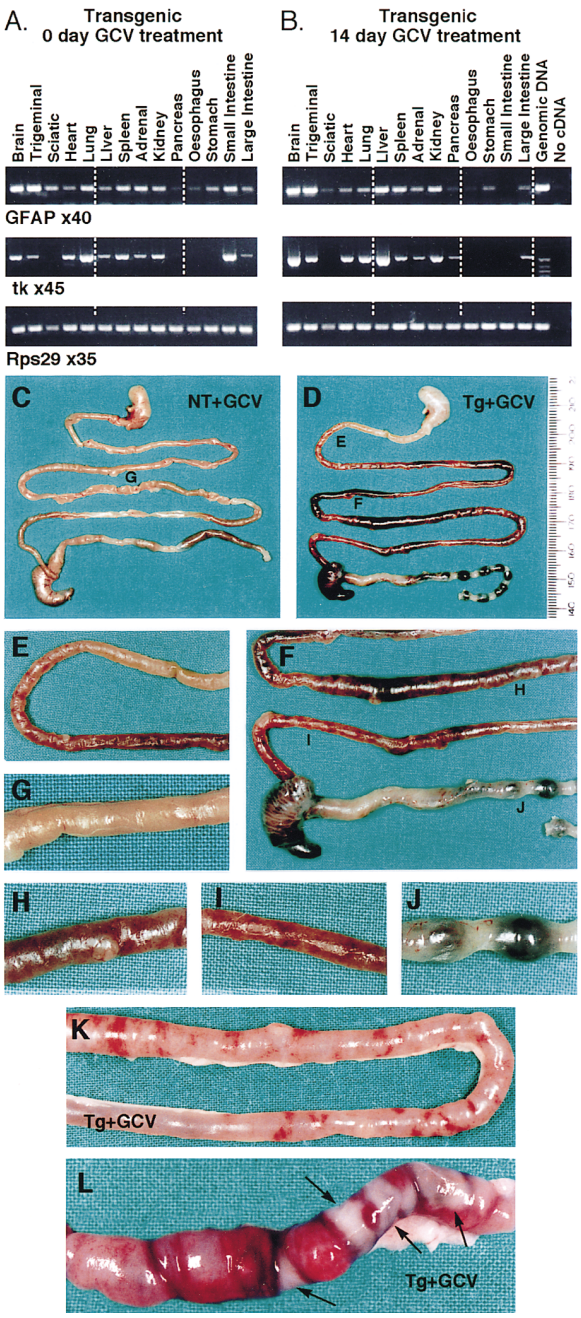

Figure 4. Effects of GCV on Expression of *Gfap* and HSV-*Tk* mRNAs, and on the Macroscopic Appearance of the GI Tract

(A and B) RT-PCR of *Gfap* and HSV-*Tk* mRNAs in untreated (A) and GCV-treated (B) transgenic mice. Even loading of cDNA for RT-PCR is shown by comparable levels of Rps29 amplification.

(C–L) Gut specimens from transgenic and nontransgenic mice treated with GCV for 11 (C–J) or 14 (K and L) days.

(C and G) Nontransgenic. GCV caused no detectable abnormalities. (D, E, F, and H–J) Transgenic. Jejunum and ileum show severe inflammation and hemorrhage (E, F, H, and I), whereas stomach (D), duodenum (E), and colon (F and J) do not. Luminal contents are dark and bloody distal to the jejunum (F, H, and I). Stool in the large bowel is normally formed but melanic (F and J). (K) Transgenic. Moderately affected ileum with scattered patches of mural inflammation and hemorrhage. (L) Transgenic. Severely affected ileum with markedly inflamed and hemorrhagic bowel wall, and ulcers with gangrenous necrosis (arrows).

6) revealed no evidence of abnormalities (Figures 4C and 4G; 5A, 5B, 5D, and 5E). In transgenic mice given GCV for 7 days (n = 6), the GI tract exhibited small patches of focal inflammation, but there were no quantitative histopathological changes (Figure 5A), and there was no occult blood in the stool. In transgenic mice given GCV for 11 or more days (n = 18), the fecal contents were black, melanic (Figures 4D, 4F, and 4H–4J), and tested positively for occult blood. Macroscopically, the jejunum and ileum exhibited severe inflammation and hemorrhage, and moderate distension; the duodenum was not affected severely, and the esophagus, stomach, and colon appeared normal (Figures 4D, 4E, 4F, and 4H–4K). There was never any evidence of stasis of gut contents, and in all cases there were normally formed stool pellets in the colon (Figures 4D, 4F, and 4J). Changes in the small bowel were patchy, appearing as skip lesions, which varied in severity from small inflammatory foci interspersed amongst normal tissue to large aphthoid and linear ulcers exhibiting gangrenous necrosis in extreme cases (Figures 4K and 4L). There was regular evidence of adhesions. The ileum was generally more severely affected than the jejunum, but within the ileum, lesions occurred with equal frequency within the proximal, central, or distal portions. The mucosal surface exhibited many areas of superficial erosion covered with inflammatory exudate and cellular debris. Microscopic analysis of the jejunum and ileum revealed a perturbed crypt-villus architecture and mucosal hyperplasia with a statistically significant 50% increase in crypt depth (Figures 5A–5G). Villus atrophy was not pronounced (Figure 5A), but villi exhibited cellular abnormalities ranging from mild epithelial changes and nonspecific granulocytic infiltrate of neutrophils and other leukocytes (Figures 5F) to marked hemorrhagic necrosis (Figure 5G). Microscopy confirmed the patchy nature of the pathology, with abnormal regions immediately adjacent to more normally appearing areas (Figures 5C). Pathology appeared to initiate in the villus tips with flattening, vacuolization, and loss of polarity of the surface epithelium, loss of the brush border and goblet cells, interstitial edema separating the epithelium from the lamina propria, and pronounced dilation of capillaries with erythrostasis (Figures 5D, 5F, and 5G; 8D, 8E, and 8G). These changes were observed frequently in the absence of hemorrhage or necrosis, whereas the reverse was not encountered. Progression of these changes included increased sloughing of epithelial cells and crypt hyperplasia, increased transmigration of polymorphonuclear leukocytes leading to granulocytic inflammatory infiltrate of the lamina propria, formation of intravascular microthrombi, and fibrosis of, and hemorrhage into, the lamina propria (Figures 5F–5H; 8E–8G). In severely affected villi, the tips had disintegrated giving rise to a hemorrhagic and inflammatory exudate into the bowel lumen (Figures 5C, 5G, and 5H). In severely affected regions, there was inflammation and hemorrhagic necrosis of the submucosa and muscularis externa, but this pathology was not observed in the absence of changes to overlying villi (Figures 5D, 5F, and 5G). There was no evidence of cryptitis or crypt abscesses (Figures 5F–5H). Some areas of severely ulcerated mucosa were associated with necrosis of the underlying muscle layer

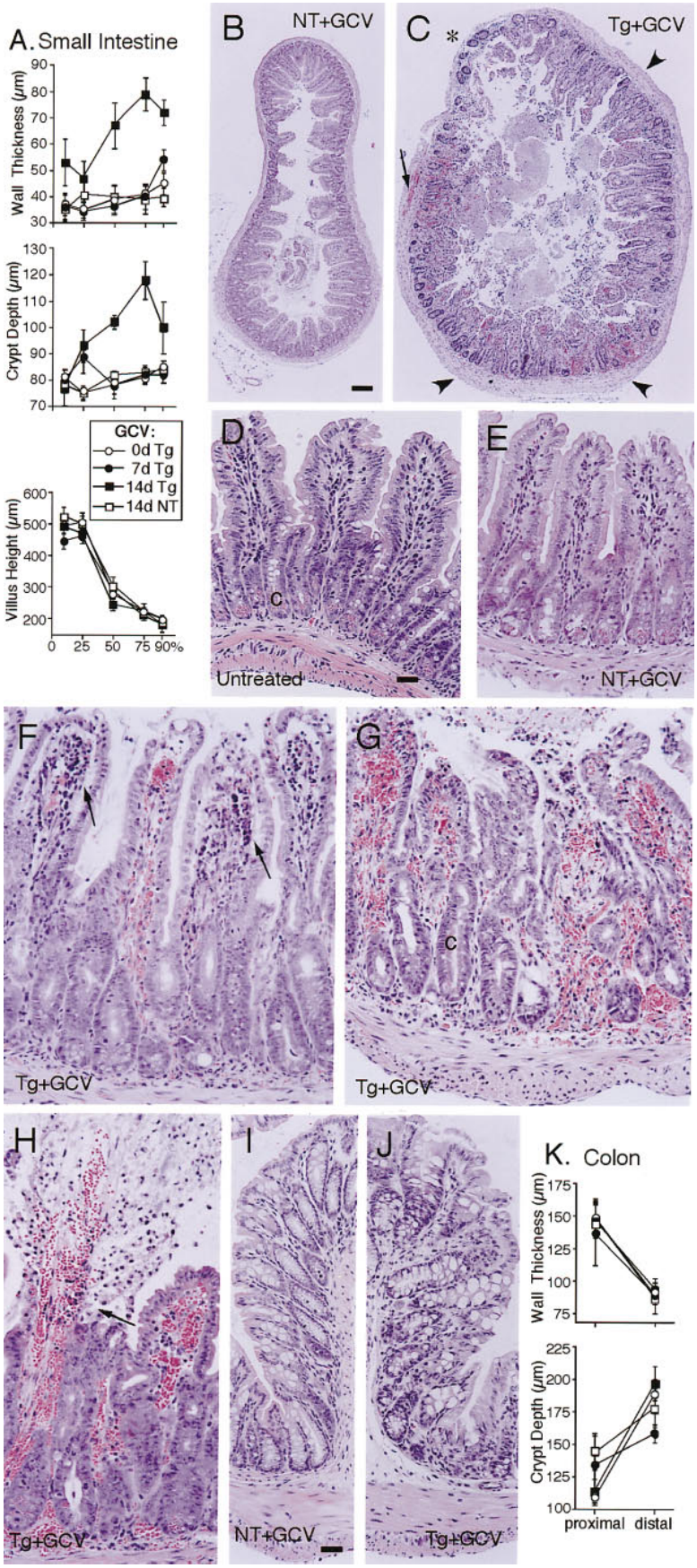

Figure 5. Histopathology of the Ileum and Colon in GCV-Treated Nontransgenic and Transgenic Mice

(A) Quantitative analysis of small intestine at five intervals (10%–90%) between the stomach and cecum in four treatment groups: transgenic mice not treated with GCV (0d Tg) or treated with GCV for 7 days or 14 days (7d Tg or 14d Tg), and nontransgenic mice treated with GCV for 14 days (14d NT). Fourteen-day Tg showed significantly greater mean muscle wall thickness and crypt depth in the mid-to-distal portion (50%–90%) portion of small intestine (corresponding to jejunum and ileum) in comparison with the other treatment groups ($p < 0.01$, Mann Whitney U-test). Mean villus height did not differ significantly in any treatment group.

(B–J) H and E-stained cross sections of ileum or colon. (B, D, and E) Ileum of GCV-treated (11 days) nontransgenic mouse (B and E) is indistinguishable from untreated (D). (C, F, G, and H) Ileum of GCV-treated (11 days) transgenic mice exhibits pronounced disruption of crypt-villus architecture, with subepithelial interstitial edema (arrows in F), mixed inflammatory infiltrate, and crypt hyperplasia (C, F, and G) and hemorrhagic necrosis of the villi and sub mucosa (G and H). The muscle wall shows regions of thickening (arrowheads in C), intramural hemorrhage (arrow in C), and degeneration beneath mucosal ulceration (asterisk in C). The bowel lumen contains hemorrhagic and inflammatory exudate (C) arising from degenerating villus tips (G, arrow in [H]). Scale bar for B and C = 140 μm, for D–H = 30 μm. (I and J) Proximal colon of GCV-treated (11 days) nontransgenic (I) and transgenic (J) mice are indistinguishable. (J) derives from the mouse shown in (G). Scale bar = 40 μm.

(K) Quantitative analysis of proximal and distal colon showed no significant difference in muscle wall thickness or crypt depth (same treatment groups as in [A]).

and transmural perforation (Figures 5C). In general, however, the smooth muscle wall exhibited a qualitatively obvious and statistically significant 100% thickening (Figures 5A–5C). Other regions of the GI tract, in particular the colon, appeared microscopically normal by qualitative and quantitative analysis (Figures 5I–5K).

Blood cell counts and serum chemistry were normal in untreated transgenic mice, in nontransgenic mice given GCV for 14 days, and in transgenic mice given GCV for 7 days. Transgenic mice with mild signs of illness after 14 days of GCV had red blood cell counts and hemoglobin levels reduced to about 60% of normal, with up to 10-fold elevations of nucleated red blood cells, up to 20-fold elevations of neutrophils, and mild (about 30%) elevations of serum urea. Moribund GCV-treated transgenic mice exhibited severe anemia with red blood cell counts and hemoglobin levels reduced to less than 25% of normal, accompanied by high levels of nucleated red cells and neutrophils relative to the number of red blood cells, and markedly elevated (>3-fold) serum urea. Mean corpuscular volume and hemoglobin, and the number of thrombocytes were in the normal range in all animals. These findings ruled out bone marrow failure. Serum creatinine and other serum chemistry values were also normal. High levels of serum urea combined with normal serum creatinine indicate normal kidney function combined with GI bleeding. Bacterial cultures prepared from blood, peritoneal fluid, and spleen showed no growth of gram-negative organisms in control mice whereas transgenic animals treated with GCV for 14 days showed >300 colonies per spleen or ml of blood or peritoneal fluid. Together, these findings were compatible with severe hemorrhage into the intestinal tract and perforation of the intestine accompanied by bacteremia as causes of acute decline and death in transgenic mice treated with GCV for 11 days or more.

Localization of HSV-TK in GFAP-Positive Enteric Glia and Preferential Loss of These Cells from Jejunum and Ileum after GCV Treatment in Transgenic Mice

To investigate the cause of gut pathology in transgenic mice receiving GCV, the cellular sites of GFAP and HSV-TK expression were identified in the GI tract by immunohistochemistry. In agreement with previous studies (Jessen and Mirsky, 1980; Gershon and Rothman, 1991), we observed GFAP-positive enteric glia in an extensive network throughout the myenteric and submucosal plexuses in whole-mount preparations and cross sections (Figures 6A and 6G). In addition, we found many GFAP-positive glia within the lamina propria, with processes that closely embraced the crypts or extended to the distal-most tips of villi (Figures 6G and 6H). GFAP immunoreactivity was not detected in other intestinal cell types. In transgenic mice, HSV-TK immunoreactivity was present in the nuclei and somata of cells with the morphological appearance of enteric glia, and double labeling confirmed that HSV-TK was present only in GFAP-positive cells (Figures 6B–6D). After 14 days of GCV treatment, there was a pronounced, but incomplete, loss of GFAP- and HSV-TK-positive cells and processes from the myenteric plexus in the jejunum and ileum, and remaining glia had abnormal morphologies (Figures 6E and 6F). Cross sections showed widespread loss of GFAP-positive glial cells and their processes from the submucosal regions and the lamina propria of villi throughout the jejunum and ileum (Figures 6I and 6J). All regions with histopathological abnormalities exhibited severe loss of glia (Figure 6J). In contrast, the colon of GCV-treated transgenic mice exhibited either a small, or no obvious, loss of immunoreactive enteric glia (Figures 6K and 6L). These findings indicate that GCV treatment caused a highly selective, severe ablation of enteric glial cells from the jejunum and ileum of transgenic mice, which correlated spatially and temporally with the severe inflammation and hemorrhagic necrosis also induced by this treatment.

Changes of Enteric Neurons in the Jejunum and Ileum of GCV-Treated Transgenic Mice

In the CNS, GFAP-positive astrocytes provide supportive and protective roles for nerve cells (Eddleston and Mucke, 1993). We therefore looked for effects that ablation of enteric glia might have on enteric neurons. Whole-mount preparations of jejunum and ileum were double-labeled for GFAP and cuprolinic blue, a specific marker for enteric neurons (Holst and Powley, 1995; Karaosmanoglu et al., 1996). In control mice ($n = 6$), myenteric neurons were completely enveloped by a dense network of glial cell processes (Figure 7C). In transgenic mice treated with GCV for 11 days or more ($n = 7$), this network was markedly depleted, with a patchy variation in severity. In areas where some glial cells remained, the neurons appeared more or less normal and were denuded of enveloping glial processes to varying degrees (Figure 7D). Where glial cells and processes were largely absent, there was evidence of neuronal atrophy and loss (Figure 7E). To investigate neuronal changes quantitatively, we conducted unbiased computer-assisted stereological analysis of whole-mount specimens prepared under standardized unstretched conditions, single-stained with cuprolinic blue. This analysis revealed statistically significant differences of 31% fewer myenteric neurons, and a 27% smaller mean cross-sectional area of remaining neurons, in the ileum of GCV-treated transgenic mice as compared with controls (Figures 7A and 7B). No qualitative or statistically significant evidence of neuronal loss or atrophy was observed in the colon of GCV-treated transgenic mice (Figures 7A and 7B). Immunohistochemistry revealed no detectable difference in the appearance or density of substance P- or tyrosine hydroxylase-immunoreactive fibers in the ileum (Figures 7F and 7G) of GCV-treated transgenic mice ($n = 6$) as compared with controls ($n = 6$). Together, these findings show that ablation of enteric glia caused a moderate and patchy, but statistically significant, degeneration of neurons intrinsic to the ileal myenteric plexus, without obvious structural changes to substance P or sympathetic innervation.

Selective Decontamination of the Digestive Tract (SDD) Prevents Bacterial Overgrowth but Not Pathological Changes and Inflammation in Jejunum and Ileum of GCV-Treated Transgenic Mice

Degeneration of enteric neurons can disrupt gut motility and cause bacterial overgrowth, which in extreme cases

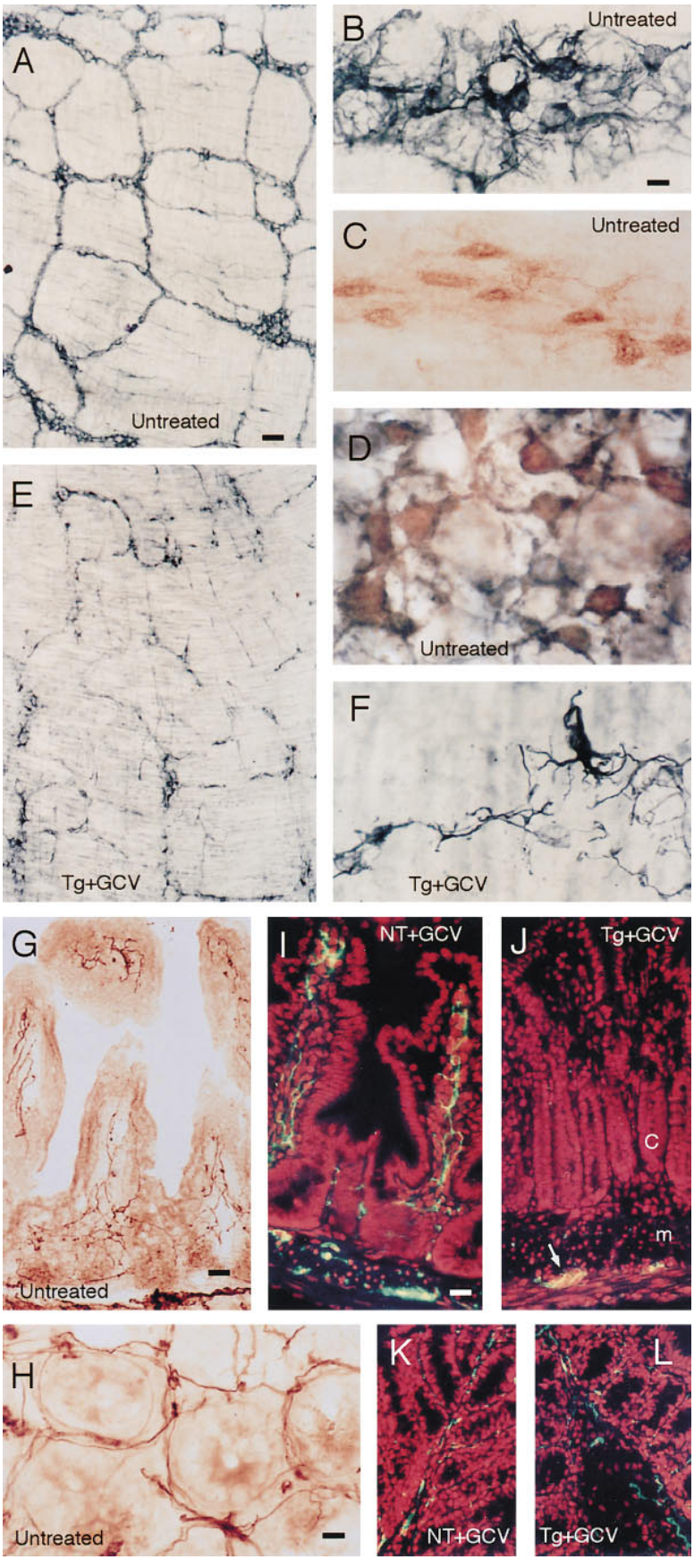

Figure 6. Cellular Localization of GFAP and HSV-TK in Ileum of Transgenic Mice before and after GCV

(A–F) Immunohistochemistry for GFAP (blue) or HSV-TK (brown) in whole-mount preparations of ileal myenteric plexus. Scale bar for (A) and (E) = 55 μm; for (B), (C), and (F) = 7 μm; for (D) = 4.5 μm.

(A–D) Untreated transgenic. GFAP-positive enteric glia and their processes extend throughout the myenteric plexus (A). In individual plexi, cells stained positively for GFAP (B) or HSV-TK (C) show similar distributions and morphologies. Double labeling shows that HSV-TK is present only in GFAP-positive cells (D).

(E and F). GCV-treated (14 days) transgenic. GFAP-positive cells and processes have been severely depleted (E), and surviving enteric glia show abnormal morphologies (F).

(G and H) Untreated nontransgenic. Immunohistochemistry of cross and tangential sections of ileum, showing GFAP-positive enteric glia and their processes throughout the lamina propria, extending to the most distal villus tips (G), and densely intertwining between crypts (H). Scale bar for G = 30 μm, for H = 20 μm.

(I–L) Confocal microscopy of immunofluorescence for GFAP (green) with propidium iodide as a nuclear counter stain (red). GFAP-immunoreactivity in the ileum is unaltered by GCV (11 days) in a nontransgenic (I) but is ablated from the lamina propria of a transgenic (J) mouse, although small amounts remain in the myenteric plexus (arrow). GFAP loss is associated with thickening of the muscle wall (m), crypt hyperplasia (c), and epithelial degeneration. GFAP-immunoreactivity in the colon shows no obvious difference in GCV-treated nontransgenic (K) and transgenic (L) mice. Scale bar for (I) and (J) = 25 μm; for (K) and (L) = 40 μm.

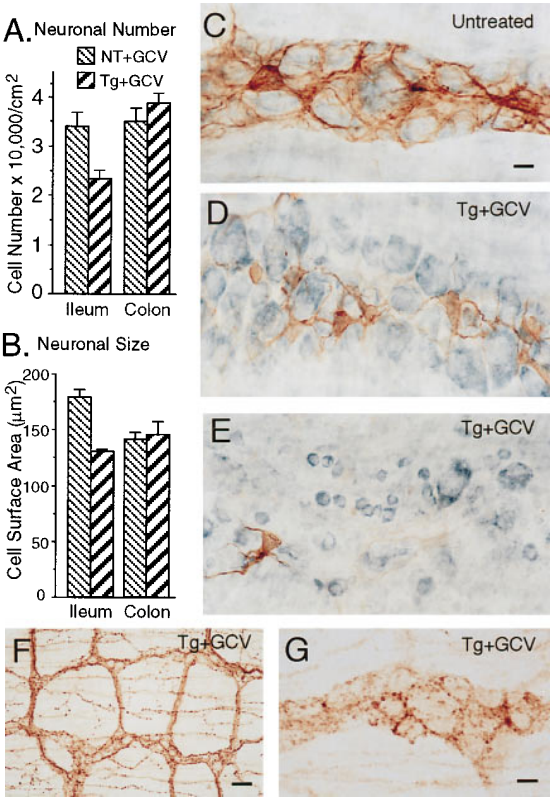

Figure 7. Effects of Ablation of Enteric Glia on Myenteric Neurons

(A and B) Mean ± SEM cell number (A) and cross-sectional area (B) of cuprolinic blue–stained myenteric neurons in whole-mount preparations of ileum or colon from GCV-treated (11–14 days) nontransgenic (NT) and transgenic (Tg) mice ($n = 6$ for all groups). Tg mice had significantly ($p < 0.001$) fewer neurons (A), and remaining neurons had a significantly ($p < 0.001$) smaller mean cross-sectional area (B). There were no significant differences in the colon.

(C–E) Immunohistochemistry of GFAP-containing glia (brown) combined with cuprolinic blue staining of neurons in whole-mount preparations of the ileal myenteric plexus. Scale bar = 10 μm.

(C) Untreated transgenic. Processes from GFAP-positive enteric glia envelope all myenteric neurons.

(D and E) GCV-treated (14 days) transgenic. In areas where some glia remain but exhibit abnormal morphologies, the neurons appear normal but are denuded of glial processes (D). In areas with near complete loss of glia, there is neuronal loss and atrophy (E).

(F and G) Immunohistochemistry of tyrosine hydroxylase (F) or substance P (G) in whole-mount preparations of ileal myenteric plexus from a GCV-treated (14 days) transgenic, showing densities of fibers and terminals indistinguishable from untreated mice. Scale bar for F = 35 μm, for G = 15 μm.

may induce inflammatory pathology in the small intestine. We therefore quantitatively assessed bacterial levels in gut segments, and examined the effects of SDD achieved with oral antibiotics, on the intestinal pathology triggered by GCV in transgenic mice. The ileum, but not duodenum or cecum, of GCV-treated transgenic mice showed statistically significant 10- to 100-fold increases in the number of anaerobic and aerobic bacterial colonies per gram tissue, respectively, as compared with untreated or GCV-treated nontransgenic mice (Figures 8A and 8B). The ileum of GCV-treated transgenic mice fed diet containing three oral antibiotics (broad spectrum, antianaerobic, and antifungal) for 14 days showed anaerobic and aerobic colony counts reduced significantly by more than 1 and 6 orders of magnitude, respectively, as compared with GCV-treated transgenic mice not receiving antibiotics (Figures 8A and 8B). Functional decontamination of the bowel was further demonstrated by a statistically significant increase ($p < 0.01$, *t* test) of cecal weight relative to body weight in mice with SDD (2.8 ± 0.5%) compared with untreated mice (1.5 ± 0.4%). Aerobic bacterial colony counts were similarly reduced in GCV-treated transgenic mice after 5 days of oral antibiotics (data not shown), indicating effectiveness of SDD during the entire period of development of the intestinal pathology in these mice.

SDD did not reduce the severity of the illness exhibited by GCV-treated transgenic mice as judged by the appearance of the mice, survival time, or severity in the reduction of hemoglobin levels. The small bowel of GCV-treated nontransgenic mice with SDD appeared normal; however, the small bowel of GCV-treated transgenic mice with SDD exhibited severe macro- and microscopic pathology with mucosal degeneration, capillary dilation, erythrostasis, granulocytic inflammatory infiltration, and hemorrhagic necrosis similar to GCV-treated transgenic mice that did not receive antibiotics (Figures 8C–8G). Standard microbiological screening and serological tests showed no evidence of contagious pathogens in these mice, such as *Clostridium*, *Salmonella*, *Yersina*, parasites, and various mouse viruses. These findings demonstrate that the pathology induced in transgenic mice by GCV was not merely the result of bacterial overgrowth in the small bowel, but they do not rule out a role for bacteria in the etiology of this pathology.

Myeloperoxidase (MPO) activity deriving from azurophilic granules of polymorphonuclear neutrophils was determined in bowel segments as a specific, quantitative measure of inflammatory response (Miller et al., 1993). GCV-treated transgenic mice with or without SDD exhibited substantial and statistically significant increases in MPO activity in ileum, but not duodenum or colon, compared with GCV-treated nontransgenic mice with or without SDD (Figure 8C). These findings show that the pathological changes of the small bowel in GCV-treated transgenic mice were associated with a pronounced inflammatory infiltrate, which was not prevented by SDD.

Discussion

Enteric glia form a large and widespread network of cells at all levels of the GI tract. Their functions are not well understood. In this study, we found that ablation of enteric glia in the jejunum and ileum of adult transgenic mice led rapidly to a fulminating enteritis with severe inflammation and hemorrhagic necrosis of these organs. Ablation of enteric glia also caused degenerative changes in neural elements of the enteric nervous system, which may have contributed to the development of the associated pathology. The macro- and histopathologic appearance of the small intestine was similar to that in experimental models of inflammatory bowel disease (IBD) in rodents and in various human conditions.

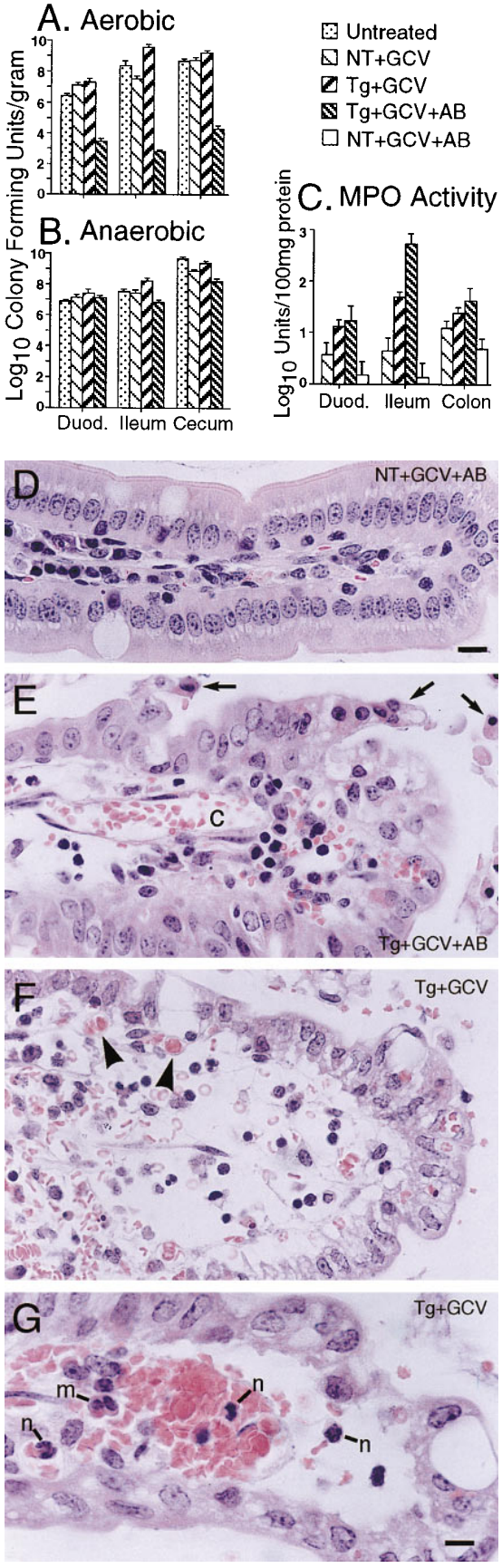

s.c. GCV Treatment Preferentially and Specifically Ablated Transgenic Glia in the Jejunum and Ileum

Most HSV-TK-expressing glial cells throughout the central, peripheral, and enteric nervous systems were not killed in detectable numbers by the regimen of GCV delivery used in this study. The reason for the preferential ablation of HSV-TK-expressing glia in the small intestine is uncertain. After phosphorylation of GCV by transgene-derived HSV-TK, GCV-mediated cell death is thought to result from the formation of toxic intermediates that disrupt DNA replication and kill proliferating cells (Frank et al., 1984; Borrelli et al., 1989). In agreement with these reports, we found that s.c. GCV treatment killed HSV-TK-expressing CNS astrocytes in vivo only adjacent to a stab injury, a procedure that induces proliferation of local reactive astrocytes. These observations suggest that different rates of cell division amongst HSV-TK-expressing glia may account for variations in their vulnerability to GCV, but other differences cannot be ruled out.

In the small intestine, HSV-TK immunoreactivity was present only in GFAP-positive enteric glia, and not in other cell types. Enteric glia were clearly ablated in the jejunum and ileum by GCV treatment, and there is no evidence to suggest that the lethal metabolites of GCV, which they produced, had any effects on neighboring intestinal cells. In previous reports, GCV treatment of transgenic mice had no toxic effects on non-HSV-TK-expressing cells that were intermingled with cells which expressed HSV-TK and died in the pituitary, thyroid, or stomach (Borrelli et al., 1989; Wallace et al., 1991; Canfield et al., 1996). In our in vitro experiments, GCV did not kill GFAP- and HSV-TK-negative cells; instead,

Figure 8. Effects of SDD on the Inflammation and Pathology Induced by GCV in Transgenic Mice

(A and B) Mean number ± SEM of aerobic (A) and anaerobic (B) colony forming units per gram tissue. GCV-treated (14 days) transgenic mice (Tg + GCV) showed significantly higher counts of both aerobic and anaerobic bacteria in ileum, but not other gut regions, compared with untreated, or GCV-treated nontransgenic (NT + GCV), mice. Tg + GCV mice given antibiotics for 14 days (Tg + GCV + AB) showed significantly fewer aerobic counts in all three gut regions, and significantly fewer anaerobic counts in ileum and cecum, compared with untreated or NT + GCV mice. ($p < 0.01$, ANOVA with Newman-Keuls post hoc pair-wise comparison).

(C) Mean value ± SEM of myeloperoxidase (MPO) activity expressed as units per 100 mg protein. Tg + GCV and Tg + GCV + AB mice showed significantly higher values in ileum but not other gut regions compared with NT + GCV mice or mice treated with NT + GCV + antibiotics (NT + GCV + AB). ($p < 0.01$, ANOVA with Newman-Keuls).

(D–G) H and E-stained cross sections of villus tips in comparable regions of midileum. Scale bar for (D)–(F) = 10 μm; for (G) = 6.3 μm. (D) NT + GCV + AB. Healthy columnar epithelium with a prominent brush border and small capillaries in lamina propria. (E) Tg + GCV + AB. Loss of brush border and epithelial polarity, increased sloughing of epithelial cells (arrows), and pronounced dilation of capillaries (c). (F) Tg + GCV. Degeneration and vacuolization of epithelium, sclerosis of lamina propria, formation of microthrombi in the capillaries (arrowheads), and extravasation of red and white blood cells. (G) Tg + GCV. Severe dilation of a capillary with erythrostasis and numerous polymorphonuclear leukocytes including neutrophils (n) and monocytes (m).

these cells increased in number while neighboring GFAP-positive, HSV-TK-expressing astrocytes died. Together, these findings indicate that lethal metabolites of GCV are not released by HSV-TK-expressing cells in sufficient quantities to kill neighboring cells, and that GCV specifically ablated enteric glia in the small intestine of our transgenic mice.

Enteric Glia Play a Fundamental Role in Bowel Function

Ablation of enteric glial cells in the jejunum and ileum led rapidly to severe inflammation and necrosis. The persistence of the pathology in mice with SDD showed that this subacute, necrotizing enteritis was not merely caused by bacterial overgrowth resulting from disturbed gut motility due to neuronal degeneration. Thus, functional changes induced by the loss of enteric glia played a primary role in triggering the disease process. To our knowledge, there are no previous reports presenting evidence for, or postulating, a direct link between the loss or dysfunction of enteric glia and pathological changes in the bowel. The sequence of events appeared to involve early breakdown of the epithelium, and microvascular disturbances. Our observations are also compatible with a role for normal gut constituents (food proteins and bacterial flora) in the inflammatory process.

The rapid induction of severe intestinal pathology after the ablation of enteric glia demonstrates that these cells play a fundamental role in maintaining the integrity of the bowel. Based on comparison with known functions of related GFAP-expressing glia in other neural systems, there are a number of ways in which enteric glia could exert powerful effects on bowel function, either by influencing enteric neurons or through direct interactions with nonneuronal cell types.

In the CNS, fibrous processes of GFAP-positive astrocytes surround and contact essentially all types of neurons. Interactions between neurons and glia via these processes show considerable plasticity and play important roles in regulating neuronal function (Theodosis and MacVicar, 1996). The denuding of myenteric and submucosal neurons of glial processes in GCV-treated transgenic mice is likely to have had a pronounced effect on their function. In other neural tissues, glia also provide important protective and/or supportive functions for neurons. In the *Drosophila* mutant *drop dead*, glial cell degeneration precedes, and is thought to cause, neuronal degeneration (Buchanan and Benzer, 1993). In the mammalian CNS, GFAP-positive astrocytes buffer neurons from the accumulation of potentially toxic endogenous molecules and produce neurotrophic growth factors (Eddleston and Mucke, 1993). Our observations demonstrate that loss or dysfunction of enteric glia leads to substantial degeneration of myenteric neurons, which may be due to loss of trophic or neuroprotective functions. Enteric glia produce glial-derived neurotrophic factor (GDNF) (Bar et al., 1997), and embryonic mice homozygous for deletion of the genes for GDNF or its receptor fail to develop enteric neurons (Moore et al., 1996; Pichel et al., 1996; Sanchez et al., 1996). Enteric neurons, like CNS neurons, are vulnerable to glutamate-mediated excitotoxicity (Kirchgessner et al., 1997), and in the CNS, disruption of glutamate uptake by astrocytes causes excitotoxic neuronal death (Rothstein et al., 1996).

Enteric glia may also influence neural fibers and projections from enteric neurons. The continuous turnover of intestinal mucosa due to epithelial sloughing requires constant remodeling of enteric neural connections. This activity is reflected in the constitutive expression by enteric neurons of GAP-43 (Sharkey et al., 1990). In the adult CNS, astrocytes support some types of sprouting or regenerating axons (Kawaja and Gage, 1991). GFAP-positive enteric glia that envelop axon bundles (Gershon and Rothman, 1991) may play a similar role, with the consequence that loss or dysfunction of enteric glia could lead to a failure of certain enteric neural projections.

The widespread distribution of enteric glia and their processes throughout the intestinal mucosa, embracing crypts and extending to the most distal villus tips, suggests that molecules released from these cells could influence many cell types. GFAP-positive glial cells in the CNS produce, and are affected by, many growth factors and cytokines and participate in inflammatory and immune responses (Eddleston and Mucke, 1993), a capacity that may be shared by GFAP-positive enteric glia (Bar et al., 1997). CNS astrocytes also induce blood-brain barrier properties in endothelia (Janzer and Raff, 1987), and some enteric glia display terminal swellings resembling the endfeet of CNS astrocytes (Gershon and Rothman, 1991), which often anchor astrocytes to blood vessels. In this context, it is interesting that ablation of enteric glia in this study caused microvascular disturbances and certain changes resembling ischemic bowel.

Changes Induced by Ablation of Enteric Glia Are Similar to IBD

The pathological changes induced in our transgenic mice by ablation of enteric glia, although subacute and fulminating in nature, bear similarities to IBD in animal models and various human conditions, in particular Crohn's disease (Strober and Ehrhardt, 1993; Sharkey and Parr, 1996). The features of IBD are of unknown etiology in human disease (Goyal and Hirano, 1996) and can be induced to varying degrees in experimental animals either by treatment with certain chemicals (Sharkey and Parr, 1996), the targeted deletion of genes for IL-2, IL-10, or T cell receptors (Kühn et al., 1993; Mombaerts et al., 1993; Sadlack et al., 1993), or the genetically targeted disruption of epithelial adhesion (Hermiston and Gordon, 1995). While these animal models strongly implicate immune and neural dysfunction in IBD, the cascade of cellular events remains uncertain.

Similarities in the appearance of end-stage pathology in various bowel conditions suggests that the gut may have limited ways of responding when it is defective. For this reason, it is important to identify single events that are able to trigger complex pathological cascades. In this study, loss or dysfunction of enteric glia played a primary role in triggering inflammatory bowel pathology, suggesting that these cells may play a role in IBD. The enteric nervous system has been implicated in IBD through partial neural degeneration combined with preservation or increases in proinflammatory peptides such

as substance P and sympathetic innervation (Goyal and Hirano, 1996; Sharkey and Parr, 1996; McCafferty et al., 1997). Our findings after ablation of enteric glia are similar. It is interesting that pronounced degenerative changes in the myenteric plexus alone do not precipitate IBD in experimental animals (Dahl et al., 1987) or in patients with Hirschsprung's disease, suggesting that imbalance of neural regulation, rather than extensive neuronal degeneration, may be important. As discussed above, the loss or dysfunction of enteric glia may have effects on bowel functions other than, and in addition to, effects on enteric neurons. We speculate that disturbances in enteric glia have the potential to represent a link between immune, vascular, and neural dysfunctions in IBD. The pathological changes induced by ablation of enteric glia in the transgenic mice described here provide a model for investigating both the etiology and potential treatments of IBD and other forms of enteritis.

Experimental Procedures

Gfap-HSV-*Tk* Fusion Gene Construct

Starting with a 15 kb *Gfap-lacZ* plasmid, the *lacZ* sequence was replaced with HSV-*Tk* sequence (Figure 1A). A 1.7 kb XbaI–Bam HI fragment, including the HSV-*Tk* gene and its polyadenylation signal, was inserted into a pBSII-KS vector (Stratagene). The insert was reexcised using Sal I and Not I and ligated into the first exon of a *Gfap* promoter cassette (clone 445) consisting of a modified murine *Gfap* gene (Johnson et al., 1995). Integrity of the HSV-*Tk* insert and flanking regions was confirmed by single-strand sequencing. The *Gfap*-HSV-*Tk* fusion gene construct was excised by digestion with SfiI and purified by gel electrophoresis.

Animals

Mice were housed in a 12 hr light/dark cycle with controlled temperature and humidity, and allowed free access to food and water. Transgenic mice were produced using standard techniques (Hogan et al., 1986). Approximately 2 pl of DNA (500 copies of linearized fusion gene construct) were pressure injected into the male pronucleus of fertilized eggs from superovulated female C57BL/10 × CBA mice mated with CFLP males (Interfauna, UK). Two-cell stage eggs were reimplanted into pseudopregnant foster mothers. DNA obtained by tail biopsy from resulting mice was digested with EcoRI and screened by Southern blot using a 1.7 kb HSV-TK probe.

Western Blot

Frozen cerebral hemispheres were freeze/thawed, homogenized in lysis buffer (20 mM HEPES [pH 7.5], 0.42 M NaCl, 1.5 mM $MgCl_2$ 0.2 mM EDTA, 0.5 mM PMSF, 0.25 mM DTT, 50 mM NaF, 1 mM sodium orthovanadate, and 20% glycerol [w/v]), and centrifuged at 10,000 g. Supernatant proteins were separated on SDS PAGE and transferred to nitrocellulose membrane. Nonspecific binding sites were blocked with 5% milk powder, followed by incubation in 1:250 rabbit anti-HSV-TK (P. Collins), 1:250 biotinylated anti-rabbit IgG (Dako), streptavidin-biotin-horseradish peroxidase complex (ABC; Vector), and diaminobenzidine (0.5 mg/ml).

In Vitro Experiments

Primary astrocyte cultures were prepared from brains of individual neonatal (<48-hr-old) littermate pups (McCarthy and de Vellis, 1980). Each culture was genotyped by Southern blot of corresponding liver DNA. Astrocyte vulnerability to GCV was assessed using the MTT (3-[4,5-Dimethylthylthiazol-2-yl]-2,5-diphenyltetrazolium bromide) assay (Hansen et al., 1989). Sister cultures were grown in triplicate in the presence or absence of 2 μM GCV for up to 7 days. For the assay, medium was replaced by MTT solution (0.5 mg/ml in PBS) for 3 hr; cells were lysed with SDS, and OD measured at 570 nm. For immunohistochemistry, cultures were fixed in 4% paraformaldehyde and stained as described below for tissue sections.

Surgical Procedures

Surgical procedures were performed under anesthesia with Avertin (0.015 ml/g) and halothane. Miniosmotic pumps were implanted subcutaneously as recommended by the manufacturer (Alzet). Stab injuries to the forebrain were made with a number 11 scalpel blade using a rodent stereotaxic apparatus (Kopf, USA).

GCV Administration

GCV (Roche, UK) was administered continuously at a rate of 100 mg/kg/day diluted in sterile physiological saline for 7, 14, or 28 days via subcutaneously implanted osmotic minipumps (Alzet, models 1007D, 2001, 2002, or 2004). This dose was reported to kill thyrocytes expressing HSV-TK in transgenic mice (Wallace et al., 1991).

Hematology, Serum Chemistry, Bacteriological Analysis

Blood was collected by cardiac puncture from animals under terminal barbiturate anesthesia. Serum chemistry, hematological analyses, and guaiac tests for occult blood in stool were conducted by the clinical laboratories of Addenbrooke's hospital, Cambridge. Aerobic bacterial cultures of blood, peritoneal fluid, or organ specimens (gut, liver, spleen, mesenteric lymph node) were prepared using either brain heart infusion or blood agar plates. Aerobic and anaerobic bacteriological analysis of the bowel was performed by BIBRA International (Surrey, UK). Segments of duodenum, ileum, and cecum in toto were homogenized in Brucella broth, plated onto blood agar plates, and grown under anaerobic or aerobic conditions.

SDD

SDD was achieved using three antibiotics incorporated into the diet (Bioserve, Frenchtown, NJ, USA): a broad spectrum antibiotic (ciprofloxacin, 0.5 mg/g), an antianaerobic agent (metronidazole, 0.25 mg/g), and an antifungal agent (fluconazole, 0.2 mg/g), which retain high concentrations in feces and are used to control bacterial number in the GI tracts of neutropenic patients. Mice consumed 3–6 g per day.

MPO Assay

MPO activity from polymorphonuclear neutrophils was assayed (Miller et al., 1993) in bowel segments (100–250 mg), homogenized, and centrifuged at 20,000 g. Pellets were resuspended, pseudoperoxidase activity negated with hexadecyltrimethlammonium bromide, followed by 3 cycles of sonication, freezing, and thawing. Supernatant (10 μl) was mixed with 90 μl of potassium phosphate buffer containing O-dianisidine dihydrochloride and H_2O_2 and absorbence determined at 450 nm. One U of MPO activity was defined as that required to degrade 1 μmol of H_2O_2 per min at 25°C. Values were expressed as MPO units per 100 mg total protein per sample.

Tissue Harvest

Mice were killed by terminal barbiturate anesthesia. Dissected tissues were either frozen in liquid nitrogen and stored at −70°C until PCR or sectioning, or fixed in 4% paraformaldehyde and processed for hematoxylin and eosin (H and E)-stained paraffin sections. Some mice were fixed by transcardiac perfusion and frozen sections prepared.

RT-PCR

Total RNA was extracted from frozen tissues and reverse transcribed. PCR primers were: *Gfap* (accession number K01347, forward GTT GTG AAG GTC TAT TCC TGG C; reverse TCC CTT AGC TTG GAG AGC AA); HSV-*Tk* (forward GGT CCC GGA TCC GGT GGT GG; reverse CGA GGC GGT GTT GTG TGG TGT); ribosomal protein S29 (Rps29, accession number L31609, forward CTG ATC CGC AAA TAC GGG; reverse GCA TGA TCG GTT CCA CTT G). Primers were used at 100 ng/reaction. Hot-lid PCR amplification of cDNA was carried out in PCR buffer containing 0.5 mM dNTPs and 0.6 U AmpliTaq DNA polymerase on PTC-225 thermal cyclers (Tetrad). PCR products were separated on agarose gel and stained with ethidium bromide.

Immunohistochemistry and Histology

Pieces of GI tract tissue, or 40 μm thick frozen forebrain sections were stained free-floating in primary antibody overnight, biotinylated

secondary antibody for 2 hr, streptavidin-biotin-horseradish peroxidase complex (ABC, Vector) for 2 hr, and diaminobenzidine (DAB, 0.5 mg/ml). For double labeling, sections were stained sequentially using DAB as a brown chromagen followed by Vector SG (Vector) to give a blue color. GFAP was also visualized using streptavidin-FITC (1:100) with propidium iodide (5 μg/ml) as a nuclear counterstain and viewed by confocal laser scanning microscopy (Bio-Rad MRC500). Rabbit primary antibody dilutions were: anti-HSV-TK 1:25,000 (P. Collins), anti-GFAP 1:25,000 (Dako); anti-TH 1:25,000 (Dako); anti-substance P 1:25,000 (Dako). Enteric neurons were visualized with cuprolinic blue alone or in combination with immunohistochemistry (Holst and Powley, 1995; Karaosmanoglu et al., 1996).

Morphometry

Smooth muscle wall thickness, crypt depth, and villus height were measured by image analysis (Seescan) in H and E-stained paraffin sections. Enteric neuron counts and cross-sectional area measurements were performed in cuprolinic blue–stained whole-mount specimens using stereology and unbiased sampling (Gundersen et al., 1988). Tissue preparations were fixed unstretched in a standardized manner. Care was taken not to introduce postmortem stretch artifacts, which might influence cell counts (Karaosmanoglu et al., 1996). Two counting frame fields (8564 μm^2) per mm^2 were selected at random using a computer-driven microscope stage (CAST, Olympus). Since whole-mount preparations are thin and unsectioned, all neurons identifiable through the depth of the specimen were analyzed per frame. At least 15 mm^2 were analyzed, at least 200 neurons were counted, and the cross-sectional area of at least 60 neurons was measured for each gut segment per animal.

Acknowledgments

We thank Dr. T. H. Rabbitts for the HSV-*Tk* plasmid; Dr. P. Collins for HSV-TK protein and antiserum; S. Jackson and Roche Products Ltd. for ganciclovir; Drs. S. Young, D. Wen-Lin, S. Murch, I. Sanderson, M. Kagnoff, and P. Sansonetti for helpful discussion; T. Humby for statistics; and J. A. Bashford, A. P. Newman and I. Bolton for photography. This work was supported by grants from The Wellcome Trust and Action Research to M. V. S. and M. H. J., and an MRC studentship to T. G. B.

Received July 23, 1997; revised March 4, 1998.

References

Al-Shawi, R., Burke, J., Jones, C.T., Simons, J.P., and Bishop, J.O. (1988). A *Mup* promoter-thymidine kinase reporter gene shows relaxed tissue-specific expression and confers male sterility upon transgenic mice. Mol. Cell. Biol. *8*, 4821–4828.

Bar, K.J., Facer, P., Williams, N.S., Tam, P.K.H., and Anand, P. (1997). Glial-derived neurotrophic factor in human adult and fetal intestine and in Hirschsprung's disease. Gastroenterology *112*, 1381–1385.

Borrelli, E., Heyman, R.A., Arias, C., Sawchenko, P.E., and Evans, R.M. (1989). Transgenic mice with inducible dwarfism. Nature *339*, 538–541.

Buchanan, R.L., and Benzer, S. (1993). Defective glia in the *Drosophila* brain degeneration mutant drop-dead. Neuron *10*, 839–850.

Canfield, V., West, A.B., Goldenring, J.R., and Levenson, R. (1996). Genetic ablation of parietal cells in transgenic mice: a new model for analyzing cell lineage relationships in the gastric mucosa. Proc. Natl. Acad. Sci. USA *93*, 2431–2435.

Dahl, J.L., Bloom, D.D., Epstein, M.L., Fox, D.A., and Bass, P. (1987). Effect of chemical ablation of myenteric neurons on neurotransmitter levels in the rat jejunum. Gastroenterology *92*, 338–344.

Eddleston, M., and Mucke, L. (1993). Molecular profile of reactive astrocytes—implications for their role in neurological disease. Neuroscience *54*, 15–36.

Frank, K.B., Chiou, J.-F., and Cheng, Y.-C. (1984). Interaction of herpes simplex virus–induced DNA polymerase with 9-(1,3-dihydroxy-2-propoxymethyl)guanine triphosphate. J. Biol. Chem. *259*, 1566–1569.

Gershon, M.D., and Rothman, T.P. (1991). Enteric glia. Glia *4*, 195–204.

Goyal, R.K., and Hirano, I. (1996). The enteric nervous system. N. Engl. J. Med. *334*, 1106–1115.

Gundersen, H.J.G., Bendtsen, T.F., Korbo, L., Marcussen, N., Moller, A., Nielsen, K., Nyengaard, J.R., Pakkenberg, B., Sorensen, F.B., Vesterby, A., and West, M.J. (1988). Some new, simple and efficient steriological methods and their use in pathological research and diagnosis. APMIS (Copenhagen) *96*, 379–394.

Hansen, M.B., Nielsen, S.E., and Berg, K. (1989). Re-examination and further development of a precise and rapid dye method for measuring cell growth/cell killing. J. Immunol. Methods *119*, 203–210.

Hermiston, M.L., and Gordon, J.I. (1995). Inflammatory bowel disease and adenomas in mice expressing a dominant negative N-cadherin. Science *270*, 1203–1207.

Heyman, R.A., Borrelli, E., Lesley, J., Anderson, D., Richman, D.D., and Baird, S.M. (1989). Thymidine kinase obliteration: creation of transgenic mice with controlled immune deficiency. Proc. Natl. Acad. Sci. USA *86*, 2698–2702.

Hogan, B., Constantini, E., and Lacy, E. (1986). Manipulating the Mouse Embryo: A Laboratory Manual (Cold Spring Harbor, New York: Cold Spring Harbor Laboratory Press).

Holst, M.C., and Powley, T.L. (1995). Cuprolinic blue (quinolinic phthalocyanine) counterstaining of enteric neurons for peroxidase imunocytochemistry. J. Neurosci. Methods *62*, 121–127.

Janzer, R.C., and Raff, M.C. (1987). Astrocytes induce blood-brain barrier properties in endothelial cells. Nature *325*, 253–256.

Jessen, K.R., and Mirsky, R. (1980). Glial cells in the enteric nervous system contain glial fibrillary acidic protein. Nature *286*, 736–737.

Johnson, W.B., Ruppe, M.D., Rockenstein, E.M., Price, J., Sarthy, V.P., Vederber, L.C., and Mucke, L. (1995). Indicator expression directed by regulatory sequences of the glial fibrillary acidic protein (*GFAP*) gene: *in vitro* comparison of distinct *GFAP-lacZ* transgenes. Glia *13*, 174–184.

Karaosmanoglu, T., Aygun, B., Wade, P.R., and Gershon, M.D. (1996). Regional differences in the number of neurons in the myenteric plexus of the guinea pig small intestine and colon: an evaluation of markers used to count neurons. Anat. Rec. *244*, 470–480.

Kawaja, M.D., and Gage, F.H. (1991). Reactive astrocytes are substrates for the growth of adult CNS axons in the presence of elevated levels of nerve growth factor. Neuron *7*, 1019–1030.

Kirchgessner, A.L., Liu, M.-T., and Alcantara, F. (1997). Excitotoxicity in the enteric nervous system. J. Neurosci. *17*, 8804–8816.

Kühn, R., Lohler, J., Rennick, D., Rajewsky, K., and Muller, W. (1993). Interleukin-10-deficient mice develop chronic enterocoloitis. Cell *75*, 263–274.

McCafferty, D.M., Wallace, J.L., and Sharkey, K.A. (1997). Effects of chemical sympathectomy and sensory nerve ablation on experimental colitis in the rat. Am. J. Physiol. *272*, G272-G280.

McCarthy, K.D., and de Vellis, J. (1980). Preparation of separate astroglial and oligodendroglial cell cultures from rat cerebral tissue. J. Cell Biol. *85*, 890–902.

Miller, M.J.S., Sadowska-Krowicka, H., Chotinaruemol, S., Kakkis, J.L., and Clark, D.A. (1993). Amelioration of chronic ileitis by nitric oxide synthase inhibition. J. Pharmacol. Exp. Ther. *264*, 11–16.

Mombaerts, P., Mizoguchi, E., Grusby, M.J., Glimcher, L.H., Bhan, A.K., and Tonegawa, S. (1993). Spontaneous development of inflammatory bowel disease in T cell receptor mutant mice. Cell *75*, 275–282.

Moore, M.W., Klein, R.D., Farinas, I., Sauer, H., Armanini, M., Phillips, H., Reichardt, L.F., Ryan, A.M., Carver-Moore, K., and Rosenthal, A. (1996). Renal and neuronal abnormalities in mice lacking GDNF. Nature *382*, 76–79.

Pichel, J.G., Shen, L., Sheng, H.Z., Granholm, A.C., Drago, J., Grinberg, A., Lee, E.J., Huang, S.P., Saarma, M., Hoffer, B.J., et al. (1996). Defects in enteric innervation and kidney development in mice lacking GDNF. Nature *382*, 73–76.

Rothstein, J.D., Dykes-Hoberg, M., Pardo, C.A., Bristol, L.A., Jin, L., Kunci, R.W., Kanai, Y., Hediger, M.A., Wang, Y., Schielke, J.P., and

Welty, D.F. (1996). Knockout of glutamate transporters reveals a major role for astroglial transport in excitotoxicity and clearance of glutamate. Neuron *16*, 675–686.

Sadlack, B., Merz, H., Schorle, H., Schimpl, A., Feller, A.C., and Horak, I. (1993). Ulcerative colitis-like disease in mice with a disrupted interleukin-2 gene. Cell *75*, 253–261.

Sanchez, M.P., Silos-Santiago, I., Frisen, J., He, B., Lira, S.A., and Barbacid, M. (1996). Renal agenesis and the absence of enteric neurons in mice lacking GDNF. Nature *382*, 70–73.

Sharkey, K.A., and Parr, E.J. (1996). The enteric nervous system in intestinal inflammation. Can. J. Gastroenterol. *10*, 335–341.

Sharkey, K.A., Coggins, P.J., Tetzlaff, W., Zwiers, H., Bisby, M.A., and Davison, J.S. (1990). Distribution of growth-associated protein B-50 (GAP-43) in the mammalian enteric nervous system. Neuroscience *38*, 13–20.

Strober, W., and Ehrhardt, R.O. (1993). Chronic intestinal inflammation: an unexpected outcome in cytokine or T cell receptor mutant mice. Cell *75*, 203–205.

Theodosis, D.T., and MacVicar, B. (1996). Neurone-glia interactions in the hypothalamus and pituitary. Trends Neurosci. *19*, 363–367.

Toggas, S.M., Masliah, E., Rockenstein, E.M., Rall, G.F., Abraham, C.R., and Mucke, L. (1994). Central nervous system damage produced by expression of the HIV-1 coat protein gp120 in transgenic mice. Nature *367*, 188–193.

Wallace, H., Ledent, C., Vassart, G., Bishop, J.O., and Al-Shawi, R. (1991). Specific ablation of thyroid follicle cells in adult transgenic mice. Endocrinology *129*, 3217–3226.